Supplemental text

Supplemental Figure legend

Figure S1. Related to Figure 2. Characterizing immediate changes in expression and chromatin accessibility

(A) Differential gene expression changes between undifferentiated HL-60 and 3 hour macrophages (321 genes), FDR < 1%, p-value < 0.01. (B and C) Differential gene expression of undifferentiated HL-60 and 6 hour neutrophils (146 genes) and monocytes (306 genes), FDR < 1%, p-value < 0.01. Representative genes are denoted by color.

(D and E) Schematic of immediate changes in gene expression. Branch lengths in diagrams represent the number of differentially expressed genes up-regulated for each cell-type at 3 and 6 hours post-differentiation. (F) Differential gene expression changes between undifferentiated HL-60 and 3 hour neutrophil (71 genes), FDR < 1%, p-value < 0.01.(G) Differential gene expression changes between undifferentiated HL-60 and 3 hour monocyte (64 genes), FDR < 1%, p-value < 0.01. (H) Differential gene expression changes between undifferentiated HL-60 and 6 hour macrophage (603 genes), FDR < 1%, p-value < 0.01. (I, J and K) Differential chromatin accessibility of early (0-24 hours) macrophage (n=465 chromatin elements), neutrophil (n=152 chromatin elements), and monocyte (n=276 chromatin elements) differentiation (p-value < 0.05). Chromatin accessibility dynamics are observed across several time-points and denoted respectively.

Figure S2. Related to Figure 3. Immediate effects of LPS-stimulation are dynamic across the transcriptome and chromatin landscape during myeloid differentiation

(A and B) Differential gene expression changes between 120-hour macrophages/neutrophils and 120-hour macrophages^{+LPS} (210 genes)/neutrophils^{+LPS} (687 genes), FDR < 1%, p-value < 0.01. Representative genes are colored and labeled for identification. FPKM values were log transformed. (C) Differential gene expression changes between 48-hour macrophages^{+LPS} (911 genes) and monocyte-derived macrophages^{+LPS} (878 genes), reflecting a majority cell-specific expression changes relative to LPS-mediated differences (FDR < 1%, p-value < 0.01). FPKM values were log transformed and n.s denotes not significant. (D) Diagram of LPS-mediated genes up-regulated and shared across all LPS treated time-points. Gene ontology analysis shows significant enrichment in terms for 16/25 genes. Red hexagon denotes enrichment in inflammatory and defense response (Benjamini < $1x10^{-7}$). Green triangle denotes enrichment in programmed cell death (Benjamini < $5x10^{-3}$). (E) Schematic design for integrative analysis of LPS-mediated changes in gene expression and chromatin accessibility. See experimental methods. (F) Cell-specific changes in differential chromatin accessibility across all myeloid cell-types, FDR < 1%, p-value < 0.01 (n=352 chromatin elements). Cluster size is denoted as (n) and colored boxes reflect cell-specific or combinatorial representation. (G) Heatmap of 237 differentially accessible LPS-mediated chromatin elements in neutrophils. Three chromatin clusters were derived using k-means. 10xRPM (Reads Per Million) values are log transformed and row-mean normalized for all data. Differential chromatin elements were associated to nearest genes (schematic, E) and shown with approximate chromatin element distance to gene TSS. Cluster size (n) is denoted. (H and H') Examples of LPS-mediated changes in chromatin accessibility and gene expression in neutrophils. Browser tracks of ATAC-seq data for neutrophils are normalized by read density. RNA-seq FPKM values are indicated for each gene and treatment. Colored boxes denote chromatin accessibility as static or dynamic. The change in gene expression and chromatin accessibility are well correlated for gene NFKBIA during LPS stimulation (top panel). Significant change in gene expression is observed for SOD2 without a significant change in promoter accessibility (bottom panel).

Figure S3. Related to Figure 3. LPS-mediated gene and open chromatin changes

(A) Differential gene expression changes between 48-hour macrophages and 48-hour macrophages^{+LPS} (115 genes), FDR < 1%, p-value < 0.01. (B) Differential gene expression changes between 48-hour macrophages^{+LPS}(27 genes) and 120-hour macrophages^{+LPS} (60 genes), FDR < 1%, p-value < 0.01. (C) Differential gene expression changes between 120-hour monocytes and 120-hour monocytes^{+LPS} (80 genes), FDR < 1%, p-value < 0.01. Representative genes are colored and labeled for identification. FPKM values were log transformed. (D) UCSC browser screenshot for S100A9 showing no change in gene expression and chromatin accessibility during LPS stimulation. ATAC-seq data for neutrophils are normalized by read density. RNA-seq FPKM values are indicated for each gene and treatment.

Figure S4. Related to Figure 6. GFI1 gene regulatory subnetwork
(A) Distribution of undifferentiated HL-60 PU.1 footprints identified by ATAC-seq that are also detected by PU.1 ChIP-seq. 4,838 (~89%) of PU.1 ATAC-seq footprints are also detected by PU.1 ChIP-seq. (B) Heatmaps of ATAC-seq read density is shown for undifferentiated HL-60 inferred PU.1 ATAC-seq footprints (Left; n=5436), PU.1 ATAC-seq footprints with a significant overlapping ChIP-seq PU.1 peak (Center; n=4,838; hypergeometric p-value < 1.3e-51), and PU.1 ChIP-seq read density for ChIP-seq PU.1 peaks with no ATAC-seq footprint detected (Right Blue heatmap; n=16,333). 10xRPM (Reads Per Million) values are log transformed and row-mean normalized for ATAC-seq and ChIP-seq data. ATAC-seq and ChIP-seq signal is shown for a window of +/-2 kb from the footprint center and ranked from strongest to weakest for all comparisons. (C) AUROC analysis of top 5,000 PU.1 ChIP-seq peaks in undifferentiated HL-60 (AUROC = 0.93). (D) GFI1 expression demonstrates a cell-specific pattern during myeloid differentiation. Maximal expression is observed in neutrophils, with minimal to no expression detected in monocyte-derived macrophages. Mean FPKM values for each time-series are shown. (E-I) GFI1 sub-circuits are shown for (E) undifferentiated HL-60, (F) neutrophil, (G) macrophage, (H) monocyte, and (I) monocyte-derived macrophages. The GFI1-MAFB interaction and GFI1 auto-regulatory feedback loop is specific to neutrophil cells. Colored edges indicate that a regulatory interaction was observed for the respective time-point. Dashed grey edges indicate regulatory interactions observed at other time-points or cell-types respectively. Colored grey gene arrows indicate no mRNA detected at a given time-point.

Figure S5. Related to Figure 5. EGR gene regulatory subnetworks
(A) Genome-view of the EGR transcription factor sub-circuitry in differentiated myeloid cells. EGR motifs are generally indistinguishable between protein family members, thus regulatory interactions are inferred from all three EGR factors (EGR1, EGR2, EGR3). (B-F) Sub-circuits of EGR regulation for (B) undifferentiated HL-60, (C) monocyte-derived macrophage, (D) monocyte, (E) macrophage, and (F) neutrophil. Our network analysis infers regulatory interactions specific to both myeloid cells and EGR members. Colored edges indicate that a regulatory interaction was observed for the respective time-point. Dashed grey edges indicate regulatory interactions observed at other time-points or cell-types respectively. Colored grey gene arrows indicate no mRNA detected at a given time-point. (G) Dynamic kinetics of EGR1 (top), EGR2 (middle), EGR3 (bottom) gene expression profiles during myeloid differentiation. We observe a rapid change in EGR expression in macrophage cells with a general increase in expression across all cells. Mean FPKM values for each time-series are shown. Colored dash lines indicate the summed expression of all EGR members for each respective time-point and cell-type.

Figure S6. Related to Figure 2. ATAC-seq data quality assessment
(A) Distribution of ATAC-seq sample efficiencies. Mean = 32%, median = 31%. (B) Histogram of consolidated ATAC-seq peaks. N= 69,658 peaks. Mean = 500bp. (C) Fraction of ATAC-seq peaks that are promoter-based (25%, +/- 1kb of TSS) or non-promoter based (75%). (D) UCSC browser screenshot of IRF3 and MAF loci emphasizing static (grey) and dynamic (red) chromatin accessibility during myeloid differentiation. Scale is 10xRPM.

Table S1. Previously validated regulatory interactions, Related to Figure 5.

Interactions	Citations
GFI Auto-regulatory Loop	1. Yücel, R., Kosan, C., Heyd, F., and Möröy, T. (2004). Gfi1: Green fluorescent protein knock-in mutant reveals differential expression and autoregulation of the growth factor independence 1 (Gfi1) gene during lymphocyte development. The Journal of Biological Chemistry *279*, 40906–40917.
EGR->GFI1	1. Chen, H., Ray-Gallet, D., Zhang, P., Hetherington, C.J., Gonzalez, D.A., Zhang, D.E., Moreau-Gachelin, F., and Tenen, D.G. (1995). PU.1 (Spi-1) autoregulates its expression in myeloid cells. Oncogene *11*, 1549–1560. 2. Okuno, Y., Huang, G., Rosenbauer, F., Evans, E.K., Radomska, H.S., Iwasaki, H., Akashi, K., Moreau-Gachelin, F., Li, Y., Zhang, P., et al. (2005). Potential autoregulation of transcription factor PU.1 by an upstream regulatory element. Mol Cell Biol *25*, 2832–2845.
EGR->PU.1	1. Laslo, P., Spooner, C.J., Warmflash, A., Lancki, D.W., Lee, H.J., Sciammas, R., Gantner, B.N., Dinner, A.R., and Singh, H. (2006). Multilineage Transcriptional Priming and Determination of Alternate Hematopoietic Cell Fates. Cell *126*, 755–766 2. Dahl, R., Iyer, S.R., Owens, K.S., Cuylear, D.D., and Simon, M.C. (2007). The transcriptional repressor GFI-1 antagonizes PU.1 activity through protein-protein interaction. The Journal of Biological Chemistry *282*, 6473–6483. 3. Spooner, C.J., Cheng, J.X., Pujadas, E., Laslo, P., and Singh, H. (2009). A Recurrent Network Involving the Transcription Factors PU.1 and Gfi1 Orchestrates Innate and Adaptive Immune Cell Fates. Immunity *31*, 576–586.
EGR Auto-regulatory Loop	1. Kubosaki, A., Tomaru, Y., Tagami, M., Arner, E., Miura, H., Suzuki, T., Suzuki, M., Suzuki, H., and Hayashizaki, Y. (2009). Genome-wide investigation of in vivo EGR-1 binding sites in monocytic differentiation. Genome Biology *10*, R41.
RUNX1->PU.1	1. Koh, C.P., Wang, C.Q., Ng, C.E.L., Ito, Y., Araki, M., Tergaonkar, V., Huang, G., and Osato, M. (2013). RUNX1 meets MLL: epigenetic regulation of hematopoiesis by two leukemia genes. Leukemia *27*, 1793–1802.
CEBPA->PU.1	1. Kummalue, T., and Friedman, A.D. (2003). Cross-talk between regulators of myeloid development: C/EBPalpha binds and activates the promoter of the PU.1 gene. Journal of Leukocyte Biology *74*, 464–470. 2. Yeamans, C., Wang, D., Paz-Priel, I., Torbett, B.E., Tenen, D.G., and Friedman, A.D. (2007). C/EBPα binds and activates the PU.1 distal enhancer to induce monocyte lineage commitment. Blood *110*, 3136–3142.
PU.1 Auto-regulatory Loop	1. Laslo, P., Spooner, C.J., Warmflash, A., Lancki, D.W., Lee, H.J., Sciammas, R., Gantner, B.N., Dinner, A.R., and Singh, H. (2006). Multilineage Transcriptional Priming and Determination of Alternate Hematopoietic Cell Fates. Cell *126*, 755–766 2. Kubosaki, A., Tomaru, Y., Tagami, M., Arner, E., Miura, H., Suzuki, T., Suzuki, M., Suzuki, H., and Hayashizaki, Y. (2009). Genome-wide investigation of in vivo EGR-1 binding sites in monocytic differentiation. Genome Biology *10*, R41.

Table S2. RNA-seq mapping and gene statistics, Related to Figure 1.

timepoint	Mapped Reads Rep1	Rep1 (Genes ≥1FPKM)	Mapped Reads Rep2	Rep2 (Genes ≥1FPKM)	Mapped Reads Rep3	Rep3 (Genes ≥1FPKM)
HL60	6154689	9741	5488706	10474	7539157	9783
3hMac	9390991	10675	13645567	10936	6672709	10653
6hMac	12653681	10865	5777659	11753	10698299	10860
12hMac	16715424	10739	4516460	10486	7845936	10690
24hMac	13177463	10389	7775620	9284	10402368	10333
48hMac	14028485	10850	11892768	10098	13040112	10887
48hMacLPS	7816972	10871	7482155	10372	6928836	9921
96hMac	11903380	11311	7033533	10195	9808073	11322
120hMac	12958949	11297	3792723	10729	9183211	11207
120hMacLPS	10115837	10321	6392176	10931	8465377	10283
3hNeu	15895154	10233	4639679	11949	9823357	10099
6hNeu	14084780	11021	5322924	12345	9703683	11044
12hNeu	13849183	11116	10701844	11597	6989124	11649
24hNeu	8321257	11040	4799889	11962	6920818	11039
48hNeu	7713569	11381	6851110	12428	7654270	11408
96hNeu	11475357	11409	5034765	12355	10172341	11369
120hNeu	10724204	10800	4673896	10197	8098747	10829
120hNeuLPS	12100881	10921	3453494	10231	8772061	10765
3hMon	22328471	10115	5052596	10656	13532706	10048
6hMon	15232215	11032	10190000	10725	11189290	10915
12hMon	13709700	10837	5612264	10612	10703588	10810
24hMon	8708230	10775	7670826	10609	7080736	10806
48hMon	9682744	10796	9500706	10343	4514870	10845
96hMon	9929608	11430	11727819	10608	8610421	11379
120hMon	6728988	10402	10183696	10311	7008633	10356
120hMonLPS	12542787	10827	14251212	10392	11654848	10421
123MonPMA	10105831	9787	13316722	10057	10088885	9754
126hMonPMA	12558612	10040	9645119	10371	10848325	10005
132hMonPMA	10878166	9752	12117241	10084	13698050	9679
144hMonPMA	10722983	9922	10419368	10324	13447850	10311
168hMonPMA	10298754	9549	10343884	10443	10198220	9511
168hMonLPS	11186064	10321	12422216	10982	14851458	10521
total (M)	373693409		261728637		306146359	

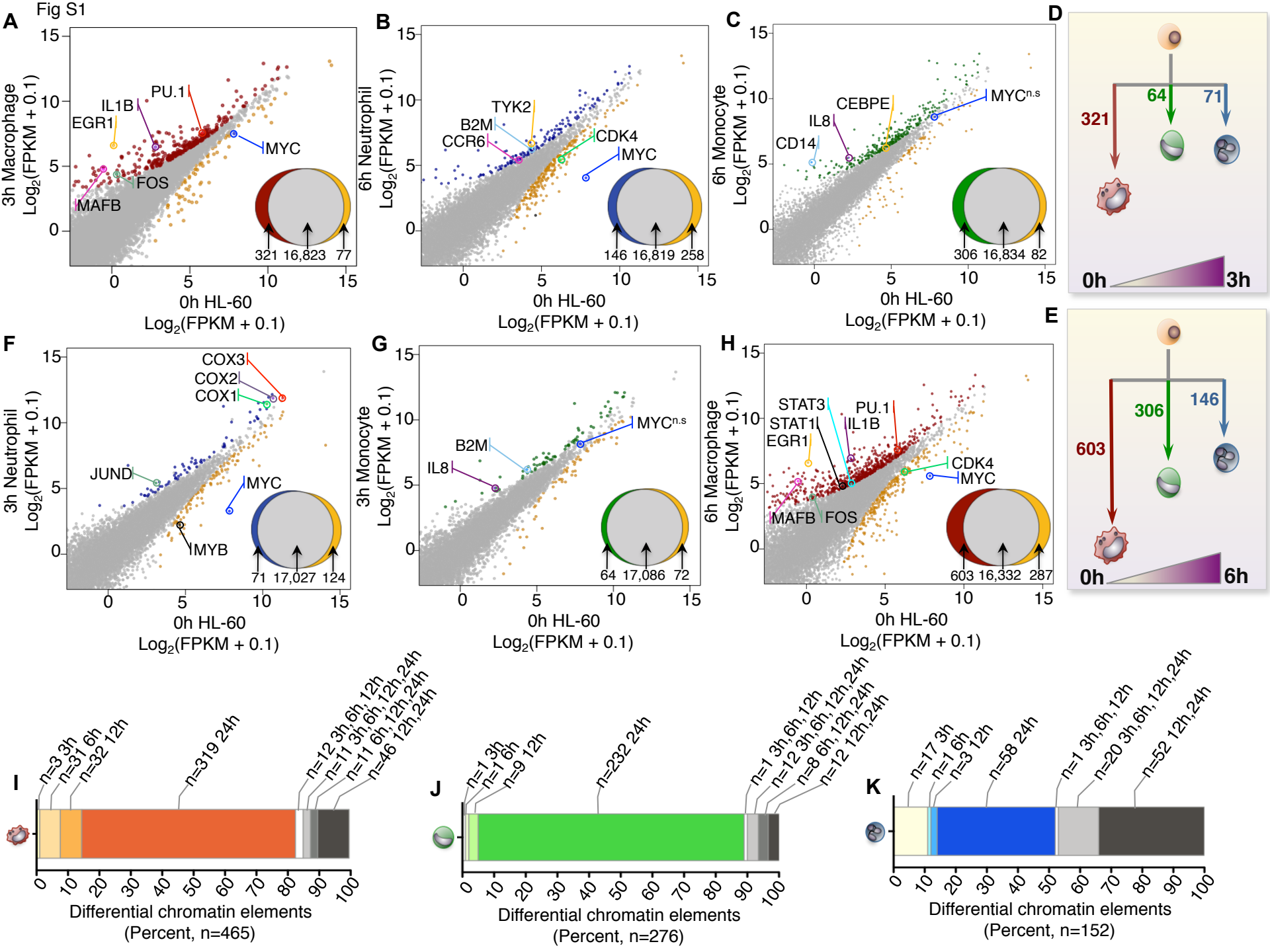
Fig S1
A
3h Macrophage Log2(FPKM + 0.1)
0h HL-60 Log2(FPKM + 0.1)
IL1B
PU.1
EGR1
MYC
FOS
MAFB
321 16,823 77
B
6h Neutrophil Log2(FPKM + 0.1)
0h HL-60 Log2(FPKM + 0.1)
TYK2
B2M
CCR6
CDK4
MYC
146 16,819 258
C
6h Monocyte Log2(FPKM + 0.1)
0h HL-60 Log2(FPKM + 0.1)
CEBPE
IL8
CD14
MYCn.s
306 16,834 82
D
321
64
71
0h
3h
E
603
306
146
0h
6h
F
3h Neutrophil Log2(FPKM + 0.1)
0h HL-60 Log2(FPKM + 0.1)
COX3
COX2
COX1
JUND
MYC
MYB
71 17,027 124
G
3h Monocyte Log2(FPKM + 0.1)
0h HL-60 Log2(FPKM + 0.1)
B2M
IL8
MYCn.s
64 17,086 72
H
6h Macrophage Log2(FPKM + 0.1)
0h HL-60 Log2(FPKM + 0.1)
STAT3
STAT1
EGR1
PU.1
IL1B
CDK4
MYC
MAFB
FOS
603 16,332 287
I
n=3 3h
n=31 6h
n=32 12h
n=319 24h
n=12 3h,6h,12h
n=11 3h,6h,12h,24h
n=11 6h,12h,24h
n=46 12h,24h
Differential chromatin elements (Percent, n=465)
J
n=1 3h
n=16 6h
n=9 12h
n=232 24h
n=1 3h,6h,12h
n=12 3h,6h,12h,24h
n=8 6h,12h,24h
n=12 12h,24h
Differential chromatin elements (Percent, n=276)
K
n=17 3h
n=1 6h
n=3 12h
n=58 24h
n=1 3h,6h,12h
n=20 3h,6h,12h,24h
n=52 12h,24h
Differential chromatin elements (Percent, n=152)

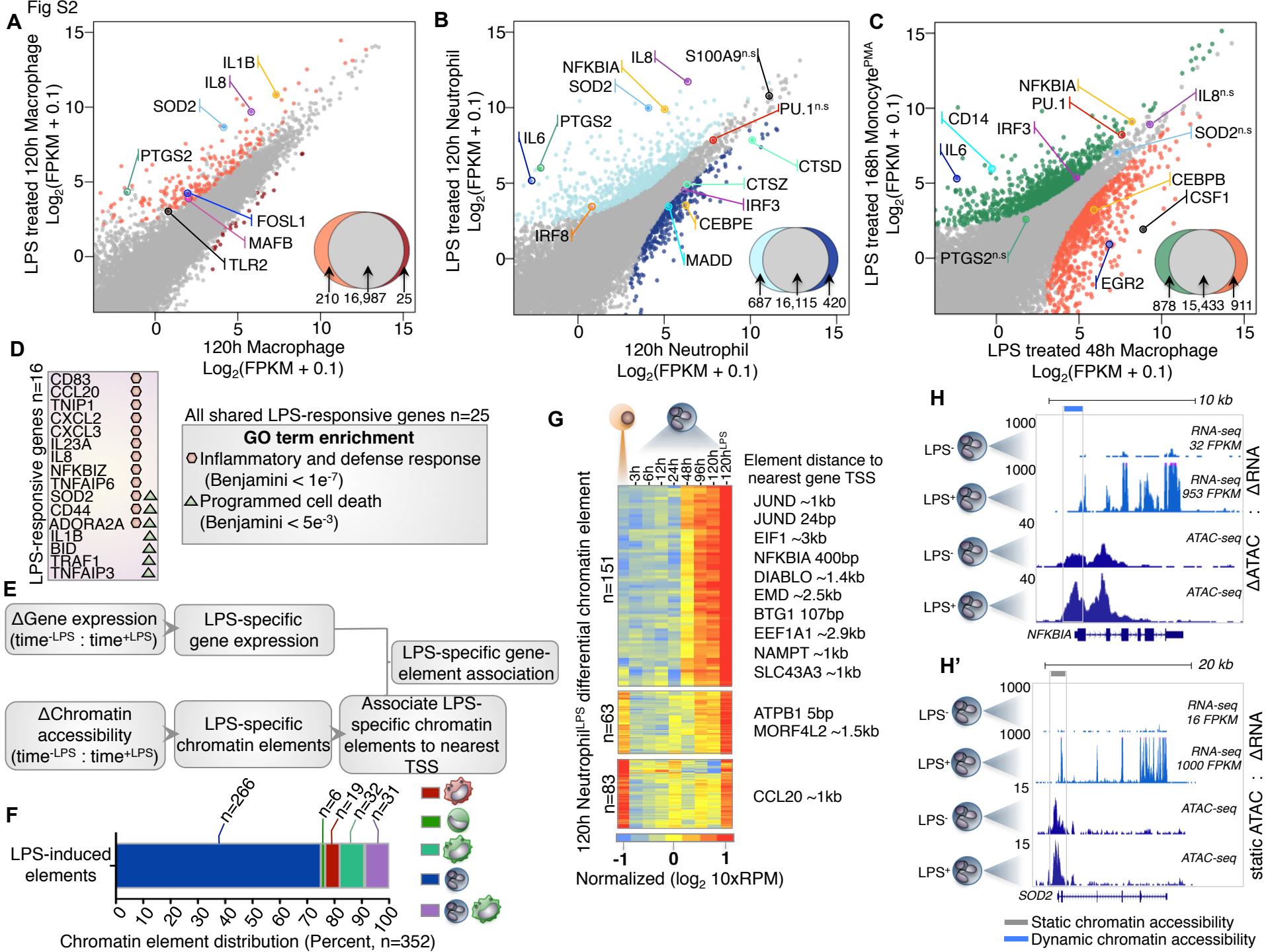
Fig S2
A
LPS treated 120h Macrophage Log2(FPKM + 0.1)
120h Macrophage Log2(FPKM + 0.1)
IL1B
IL8
SOD2
PTGS2
FOSL1
MAFB
TLR2
210 16,987 25
B
LPS treated 120h Neutrophil Log2(FPKM + 0.1)
120h Neutrophil Log2(FPKM + 0.1)
NFKBIA
IL8
S100A9n.s
SOD2
PU.1n.s
PTGS2
IL6
CTSD
CTSZ
IRF3
CEBPE
IRF8
MADD
687 16,115 420
C
LPS treated 168h MonocytePMA Log2(FPKM + 0.1)
LPS treated 48h Macrophage Log2(FPKM + 0.1)
NFKBIA
PU.1
IL8n.s
CD14
IRF3
SOD2n.s
IL6
CEBPB
CSF1
PTGS2n.s
EGR2
878 15,433 911
D
LPS-responsive genes n=16
CD83
CCL20
TNIP1
CXCL2
CXCL3
IL23A
IL8
NFKBIZ
TNFAIP6
SOD2
CD44
ADORA2A
IL1B
BID
TRAF1
TNFAIP3
All shared LPS-responsive genes n=25
GO term enrichment
Inflammatory and defense response (Benjamini < 1e-7)
Programmed cell death (Benjamini < 5e-3)
E
ΔGene expression (time-LPS : time+LPS)
LPS-specific gene expression
LPS-specific gene-element association
ΔChromatin accessibility (time-LPS : time+LPS)
LPS-specific chromatin elements
Associate LPS-specific chromatin elements to nearest TSS
F
LPS-induced elements
n=266
n=6
n=19
n=32
n=31
Chromatin element distribution (Percent, n=352)
G
120h NeutrophilLPS differential chromatin element
n=151
n=63
n=83
-3h
-6h
-12h
-24h
-48h
-96h
-120h
-120hLPS
Normalized (log2 10xRPM)
Element distance to nearest gene TSS
JUND ~1kb
JUND 24bp
EIF1 ~3kb
NFKBIA 400bp
DIABLO ~1.4kb
EMD ~2.5kb
BTG1 107bp
EEF1A1 ~2.9kb
NAMPT ~1kb
SLC43A3 ~1kb
ATPB1 5bp
MORF4L2 ~1.5kb
CCL20 ~1kb
H
10 kb
LPS-
LPS+
RNA-seq 32 FPKM
RNA-seq 953 FPKM
ATAC-seq
NFKBIA
ΔRNA : ΔATAC
H'
20 kb
RNA-seq 16 FPKM
RNA-seq 1000 FPKM
SOD2
static ATAC : ΔRNA
Static chromatin accessibility
Dynamic chromatin accessibility

Fig S3

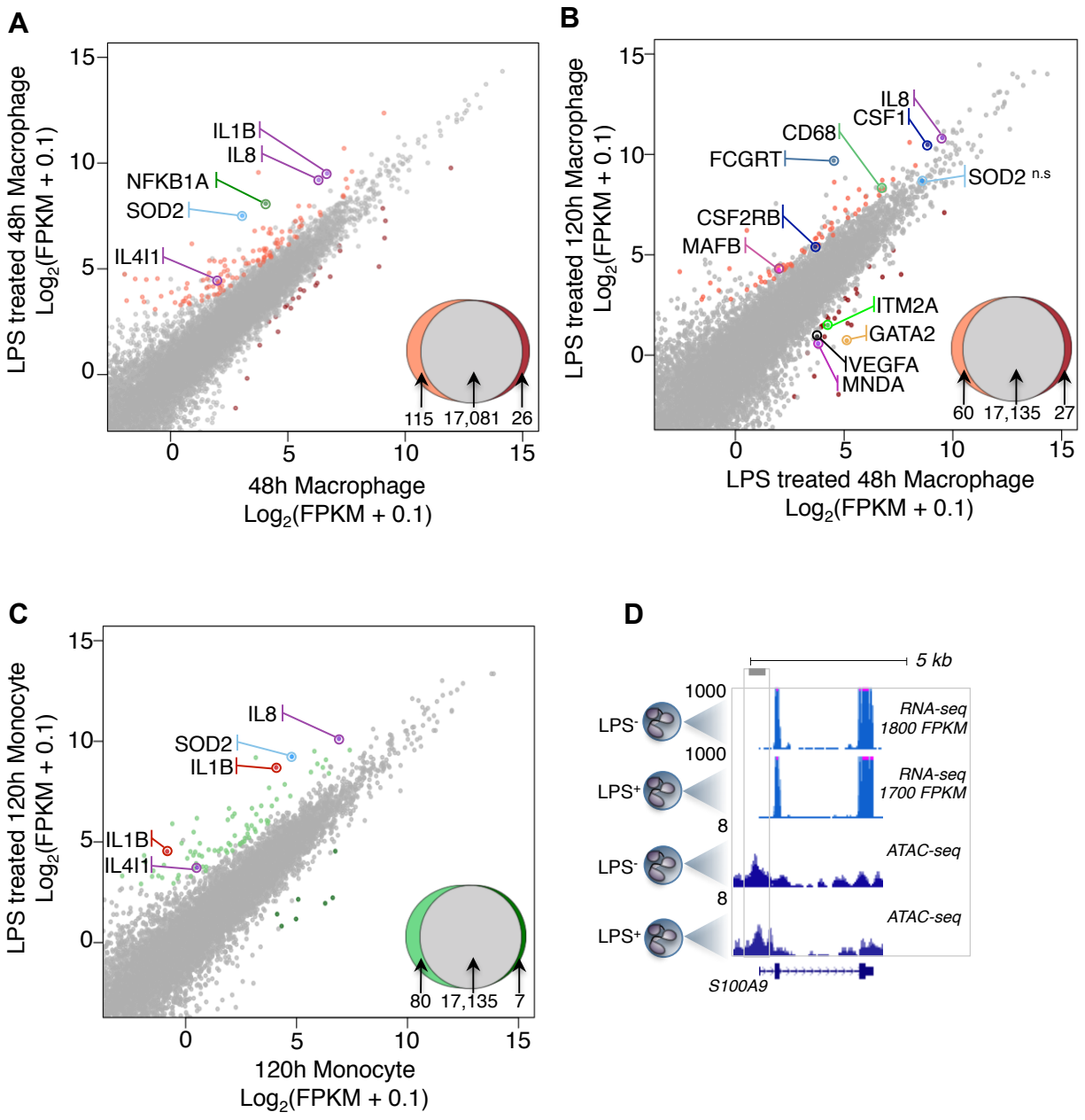
A
LPS treated 48h Macrophage
Log2(FPKM + 0.1)
48h Macrophage
Log2(FPKM + 0.1)
IL1B
IL8
NFKB1A
SOD2
IL4I1
115 17,081 26
B
LPS treated 120h Macrophage
Log2(FPKM + 0.1)
LPS treated 48h Macrophage
Log2(FPKM + 0.1)
IL8
CSF1
CD68
FCGRT
SOD2 n.s
CSF2RB
MAFB
ITM2A
GATA2
VEGFA
MNDA
60 17,135 27
C
LPS treated 120h Monocyte
Log2(FPKM + 0.1)
120h Monocyte
Log2(FPKM + 0.1)
IL8
SOD2
IL1B
IL1B
IL4I1
80 17,135 7
D
5 kb
LPS-
LPS+
1000
1000
8
8
RNA-seq
1800 FPKM
RNA-seq
1700 FPKM
ATAC-seq
ATAC-seq
S100A9

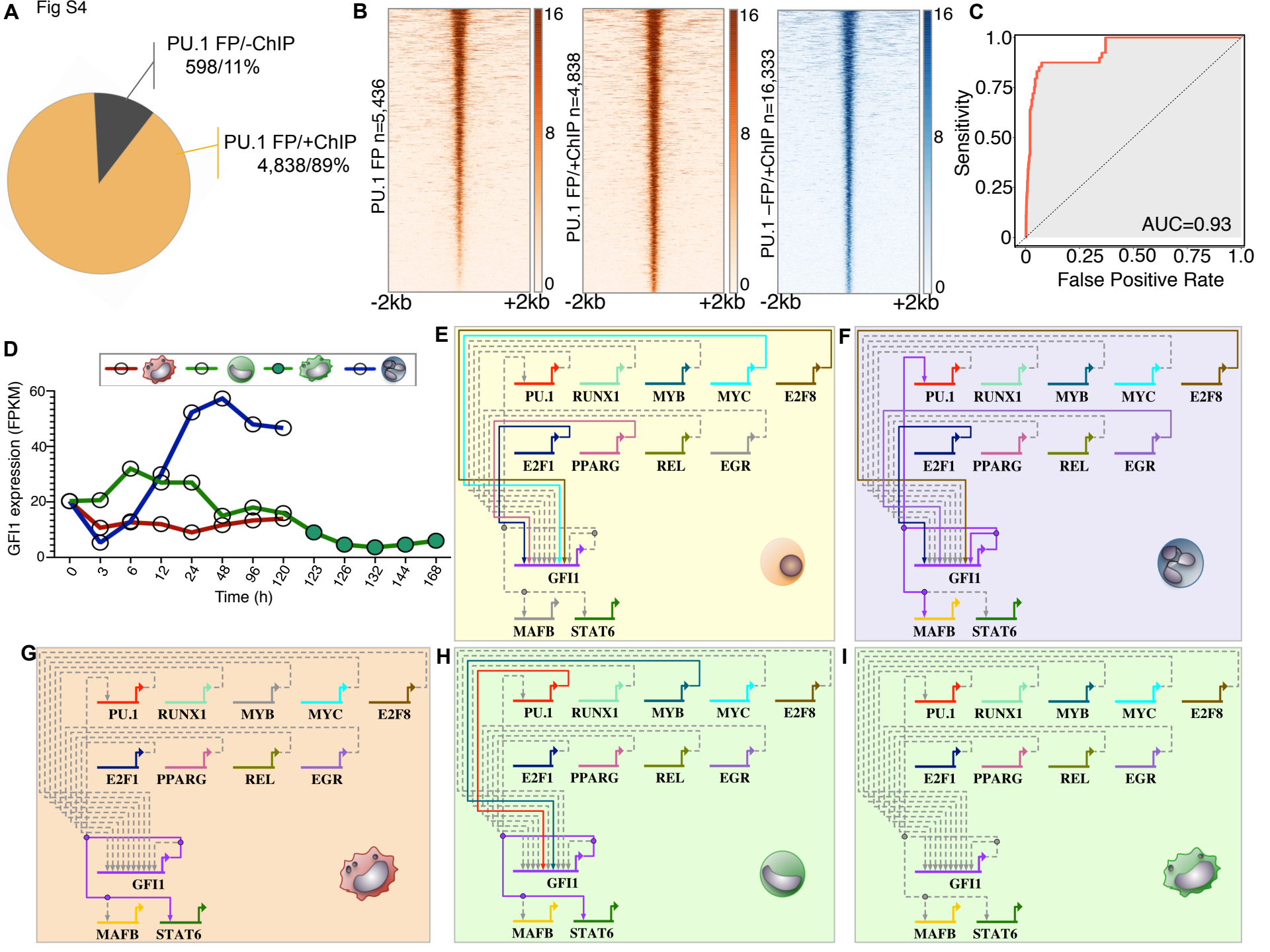
A
Fig S4
PU.1 FP/-ChIP
598/11%
PU.1 FP/+ChIP
4,838/89%
B
PU.1 FP n=5,436
PU.1 FP/+ChIP n=4,838
PU.1 –FP/+ChIP n=16,333
16
8
0
-2kb
+2kb
C
Sensitivity
False Positive Rate
AUC=0.93
D
GFI1 expression (FPKM)
Time (h)
E
F
G
H
I
PU.1
RUNX1
MYB
MYC
E2F8
E2F1
PPARG
REL
EGR
GFI1
MAFB
STAT6

Fig S5

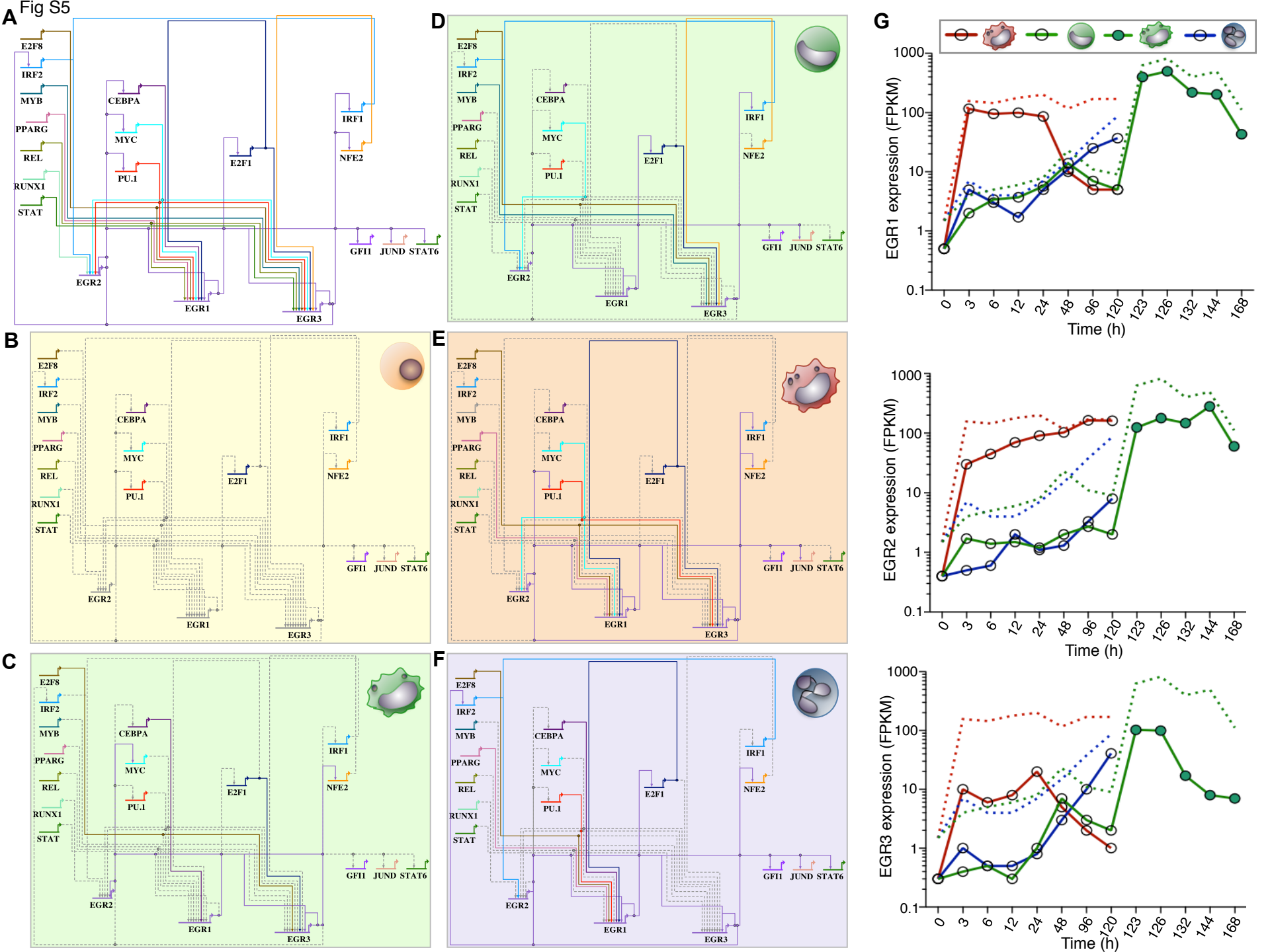
A
B
C
D
E
F
G
E2F8
IRF2
MYB
PPARG
REL
RUNX1
STAT
CEBPA
MYC
PU.1
E2F1
IRF1
NFE2
GFI1
JUND
STAT6
EGR2
EGR1
EGR3
EGR1 expression (FPKM)
EGR2 expression (FPKM)
EGR3 expression (FPKM)
Time (h)
0
3
6
12
24
48
96
120
123
126
132
144
168
0.1
1
10
100
1000

Fig S6

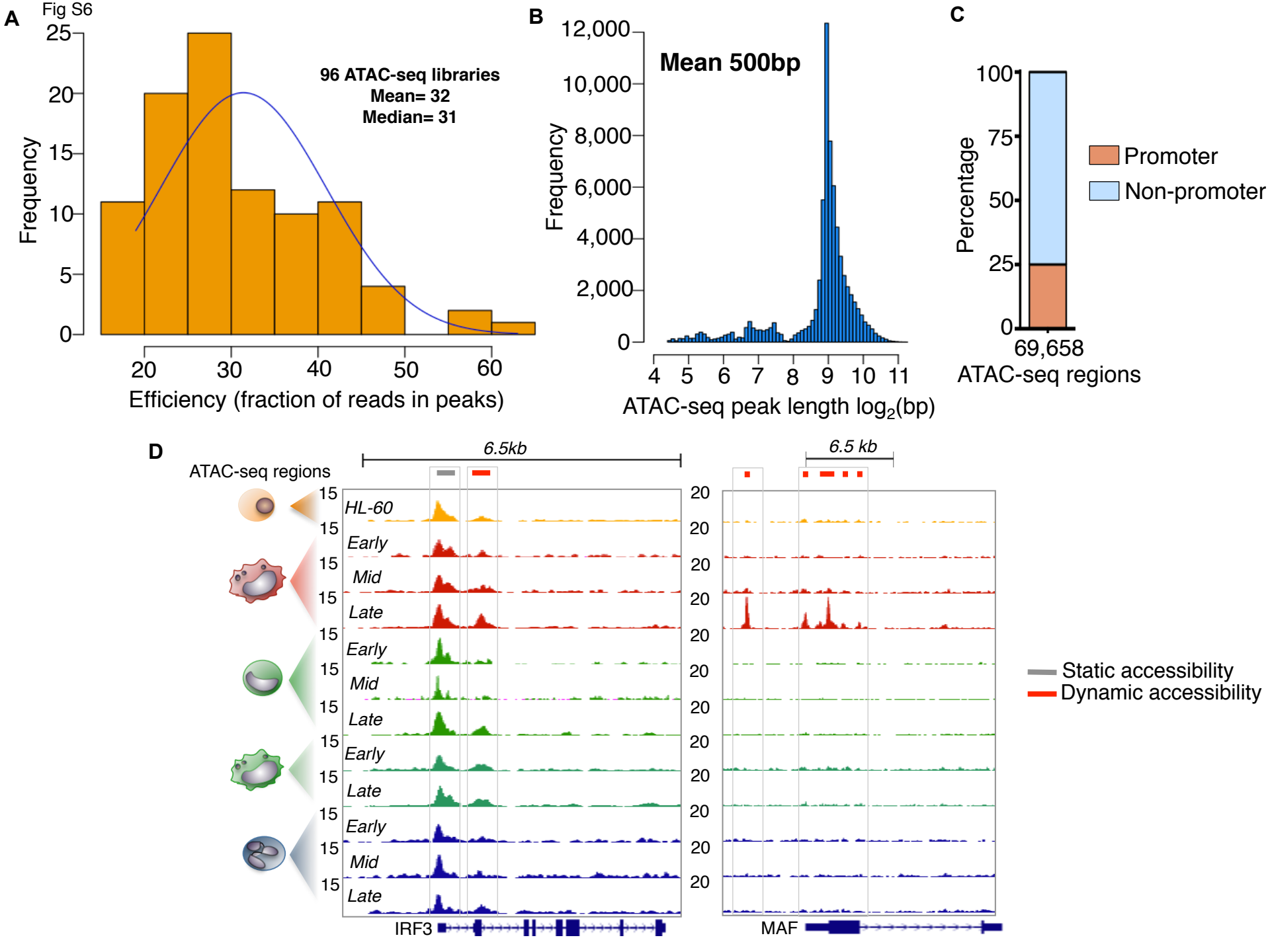
A
Frequency
96 ATAC-seq libraries
Mean= 32
Median= 31
Efficiency (fraction of reads in peaks)
B
Mean 500bp
Frequency
ATAC-seq peak length log2(bp)
C
Percentage
Promoter
Non-promoter
69,658
ATAC-seq regions
D
ATAC-seq regions
6.5kb
6.5 kb
HL-60
Early
Mid
Late
Early
Mid
Late
Early
Late
Early
Mid
Late
IRF3
MAF
Static accessibility
Dynamic accessibility